Recent Status of Thin Film Analyses by XPS

Hideo Iwai,[1*] John S. Hammond[2] and Shigeo Tanuma[1]
[1]National Institute for Materials Science, 1-2-1 Sengen, Tsukuba, 305-0047, Japan
[2]Physical Electronics USA, 18725 East Drive Lake, Chanhassen MN 55317, USA
[*]IWAI.Hideo@nims.go.jp

(Received: January 9, 2009; Accepted: February 17, 2009)

The application of XPS for film thickness analyses of overlayer thin films, the structure analysis of multilayered thin films, the background shape analyses of thin films of varying depth distributions and the compositional depth profiling by ARXPS utilizing the maximum entropy method are described. The destructive depth profiling of organic thin films (such as ~100 nm in thickness) by cluster ion beams is also described. The film thickness analysis is applied for samples such as the oxide thickness distribution on 200 mm silicon wafers. The structure analysis has a great opportunity for applications on chemically modified surfaces. The background shape analysis is useful for both homogeneous and structured thin films. The MEM applied to ARXPS data is also useful for structured analysis for such as SiON thin films. However both background shape analysis and MEM need optimizations of the parameters using prior information about the films. On the other hand, depth profiling of organic thin films in 100 nm order thickness is successfully applied with 10 keV C_{60} ion beam sputtering and with 0.2 keV Ar ion beam and 10 keV C_{60} ion beam co-sputtering.

1. Introduction

X-ray photoelectron spectroscopy (XPS) is widely used for the characterization of surfaces of materials, e.g. nanoscale advanced materials, electrodes of fuel cells, photocatalysts, etc. For both conductive and nonconductive samples, XPS can meet the strong requirement for chemical state analyses. The measurement of the thickness of a surface film is also a common requirement met with XPS [1]. For example, as the equivalent oxide thickness of state-of-the-art gate oxide is now less than 1 nm, characterization of the chemical composition and depth distribution within the gate oxide has become extremely important to understand electronic properties. The leakage current from tunneling has also increased with the reduction in traditional SiO_2 gate oxide film thickness. The development and characterization of high-k materials such as hafnium oxide has therefore received considerable attention [2]. One desire for the analysis of these materials is the elemental depth profiles within these thin films. For these analyses, the maximum entropy method (MEM) has been explored to estimate the depth distribution from the measurement results of angle-resolved XPS (ARXPS) [3-5].

Lateral inhomogeneities and sample roughness should also be considered for depth profile analyses of thin films such as self-assembled monolayers (SAM). The estimation of the background generated by energy loss of electrons from the photoelectron peak has also been applied if the thickness of the thin film is sufficiently less than approximately 3 times the inelastic mean free path of the observed photoelectron peak [6].

On the other hand, the ISO18115 has defined a thin film as typically less than 100 nm in thickness, deposited or grown on a substrate [7]. When the thickness of the thin films on a substrate approaches this thickness, a sputter etching method is generally applied to evaluate the elemental composition profile and ideally the chemical states of these elements. However severe chemical state damage can occur for both inorganic oxides and organic materials sputtered by Ar^+ ion beam irradiation. Recently the cluster ion beam has become commercially available, and has been utilized for XPS depth profiling of many organic materials to minimize the damage on the remaining surface after sputtering [8-11].

In this report, the authors will describe several of the XPS analytical techniques for thin film analyses. This overview will include non-destructive film thickness analysis, structure analysis by two emission angles, background shape analysis, depth distribution analysis from ARXPS, and depth profiling with cluster ion beams. The details of each method will be referred to other articles [for example ref.12].

2. Film Thickness Analysis

The measurement of film thickness from overlayer thin films was proposed by Hill et al (so called Hill's equation) in 1970's when the thin film is homogeneous [13]. The thickness is calculated from the ratio of the peak intensity of

photoelectrons emitted from the overlayer thin film and from the substrate. The inelastic mean free path (IMFP) for the peak from the substrate and that from overlayer thin film are assumed to be the same in Hill's equation. The kinetic energy of elemental or metallic state of photoelectron peak from the substrate is almost same as that of oxide state photoelectron peak from the overlayer thin film, as is case for the SiO_2 gate oxide of a silicon based semiconductor. The elemental Si 2p peak and oxide Si 2p peak can be extracted by curve fitting the measured Si 2p peak. The thickness t of the oxide layer is expressed in equation (2-1) [14], when the sub-oxides near the interface between oxide layer and substrate are ignored.

$$t = L_{SiO_2} \cos\theta \ln\left[1 + \frac{\left(I_{SiO_2} / R_{SiO_2}\right)}{\left(I_{Si}\right)}\right] \quad (2\text{-}1)$$

Here L_{SiO_2} is the attenuation length of Si 2p photoelectrons in a SiO_2 layer. The L_{SiO_2} values for Mg Kα X-ray and Al Kα X-ray are 2.964 nm and 3.448 nm, respectively [15], θ is the emission angle of the photoelectron with respect to the surface normal, I_{SiO_2} is the peak intensity of oxide state Si 2p, I_{Si} is the peak intensity of metal state Si 2p, and R_{SiO_2} is the intensity ratio of the bulk Si oxide to the bulk Si, which is 0.9329 [14].

Cumpson proposed a simple method of IMFP correction for two XPS peaks at different energies as equation (2-2) [16].

$$\left(\lambda_O / \lambda s\right) = \left(E_0 / E_s\right)^{0.75} \quad (2\text{-}2)$$

where λ_O and λ_s are the inelastic mean-free path (IMFP) values for oxide state Si and substrate Si, and E_O and E_S are the photoelectron kinetic energies from oxide and substrate. Cumpson extended the usefulness of the thin film analysis approach when he also proposed a simple and ease-to-use graphical method called a Thickogram [16]. These approximations can be used in the range of $0 \le \theta \le 60°$ for kinetic energies $\ge$ 100 eV for low atomic number overlayer films, and for kinetic energies $\ge$ 500 eV for all atomic numbers overlayer films [17, 18].

The International Technology Roadmap for Semiconductors (ITRS) indicates a need for the thickness measurement of gate oxides with a relative standard deviation just over 1 %. The accuracy of measurements of SiO_2 layers < 8 nm thickness on Si wafers have been assessed by 31 laboratories in 11 countries under the auspices of Consulting Committee for Amount of Substrate (CCQM). A summary of the results have been reported by Seah et al. [19-22]. The measured SiO_2 thickness values extrapolate linearly to zero. However if the predictive equation TPP-2M [23] has to be used for determining the attenuation lengths, the attenuation length uncertainties may be may around 20 %. Therefore, to achieve a thickness relative standard deviation better than 1% uncertainty for other materials, the XPS attenuation lengths should be determined by other methods such as ellipsometry, or Grazing Incidence X-ray Reflectometry (GIXRR) [19].

3. Structure Analysis

In depth composition analysis for samples such as SAMs, it is important to determine the relative order of the layers above the substrate or the relative position of different functional groups such as C=O, NO_2, etc within a particular layer. Seah et al. proposed a simple method to estimate the layer order by measuring the change of peak intensity ratios of components at two emission angles (recommended at 0 and more than 70 degrees relative to the sample normal) [24]. This method, so called structure analysis [25], can also estimate the layer thicknesses and compositions based on the estimated layer order. Here, the intensities of component "A" at lower and higher emission angles are $I_A^{\theta_L}$ and $I_A^{\theta_H}$, respectively. Similarly, the intensities of component "B" at lower and higher emission angles are $I_B^{\theta_L}$ and $I_B^{\theta_H}$ respectively. Then the ratio R is calculated as equation (3-1).

$$R = \frac{I_A^{\theta_H} / I_B^{\theta_H}}{I_A^{\theta_L} / I_B^{\theta_L}} \quad (3\text{-}1)$$

If R is larger than 1, component "A" is located above component "B" when the effective attenuation length (EAL) is almost same for each component. The positional relationship of all components can be estimated by this procedure. If R is close to 1, these components would be in the same layer.

Then, based on the estimation of layer order, iterated calculations are performed using equation (3-2) to minimize the difference between calculated and measured intensities by changing the compositions and thickness of each layer [25].

$$\frac{I_n}{I_{n+1}} = \frac{s_n t_n \lambda_{n+1,n+1}}{s_{n+1} t_{n+1} \lambda_{n,n}} \times \exp\left[\frac{1}{\cos\theta}\left(\frac{t_n + \ldots + t_1}{\lambda_{n+1,n+1}} - \frac{t_{n-1} + \ldots + t_1}{\lambda_{n,n}}\right)\right] \quad (3\text{-}2)$$

Here I_n is the intensity of nth layer from the top layer, s_n is the average relative sensitivity factor of

Table 1 Rules to estimate the depth profile from A_p/B_1, where B_1 is the parameter to give same intensity of $J(E)$ at exactly 30 eV below the peak energy and A_p is the peak area of photoelectron peak [27].

A_p/B_1	Depth distribution
$\approx 25\,eV$	Uniform
$> 30\,eV$	Surface localized
$< 20\,eV$	Subsurface localized
If the same peak from two samples has the values $D_1 = (A_p/B_1)_1$ and $D_2 = (A_p/B_1)_2$ then if $30\,eV < D_1 < D_2$ atoms are surface localized in both samples and the atoms are at more shallow depths in sample 2 than in sample 1	
if $D_1 < D_2 < 20\,eV$	atoms are in the bulk samples of both samples and at deeper depths in sample 1 than in sample 2

the component in the nth layer, t_n is the thickness of the n th layer, $\lambda_{n,m}$ is the EAL of the photoelectron which is produced in nth layer and can loose energy in m th layer. The EAL can be estimated from equation (2-2). This calculation neglects the change of atomic relative sensitivity factors of elements due to chemical shifts. This method can be applied to thin films which have a thickness which is less than a few times the EAL of the photoelectrons.

4. Background Shape Analysis

The spectral background at lower kinetic energies of the photoelectron peak is generated by inelastic scattering of photoelectrons in the bulk. The background intensity becomes higher if the photoelectrons are generated deeper in the sample. Tougaard described the inelastic scattering cross-sections using a universal function. For most metals, their oxides and alloys, the energy distribution photoelectron $F(E)$ and the observed spectrum after transmission correction $J(E)$ are expressed using a two-parameter Universal cross-section shown in equation (4-1) [26].

$$F(E) = J(E) - \int_E^\infty \frac{B(E'-E)}{\{C + (E'-E)^2\}^2} J(E')dE' \quad (4\text{-}1)$$

where $B = 2866\,eV^2$ and $C = 1643\,eV^2$.

For solids such as the light metals Al and Si, a simple two-parameter Universal cross-section is difficult to describe sharp plasmon structures, however a three-parameter Universal cross-section expressed as equation (4-2) can describe sharp plasmon structures sufficiently.

$$F(E) = J(E) - \int_E^\infty \frac{B(E'-E)}{\{C - (E'-E)^2\}^2 + D(E'-E)^2} J(E')dE' \quad (4\text{-}2)$$

where the three parameters B, C and D have been determined for different materials, e.g. polymers, SiO_2, Si, Ge, and Al [26]. B is generally adjusted to give the same intensity of $J(E)$ at the end of the background.

It is not possible to evaluate the chemical composition in depth from a sample with a non-homogeneous surface coverage using equations 4-1 and 4-2. However Tougaard has demonstrated that depth profiles estimated from the background calculations are in good agreement with the depth distributions of the real samples produced as homogeneous and exponential depth profiles, box shaped profiles (overlayer, substrate and sandwich), and island structures [27, 28]. For sandwich profiles, equation (4-1) is expressed as equation (4-3).

Table 2 Rules to estimate the depth profile from L [27].

L	Depth distribution
$-6\lambda_i < L < 6\lambda_i$	Approximately constant
$-3\lambda_i < L < 0$	Surface localized
$0 < L < 3\lambda_i$	Subsurface localized
If the same peak from two samples has values L_1 and L_2, then if $0 < L_1 < L_2 < 3\lambda_i$	atoms are surface localized in both samples and the atoms are at more shallow depths in sample 2 than in sample 1
if $-3\lambda_i < L_1 < L_2 < 0$	atoms are in the bulk samples of both samples and at deeper depths in sample 1 than in sample 2

$$F(E) = J(E) - B_1 \int_E^{\infty} \frac{E'-E}{\left\{1643 + (E'-E)^2\right\}^2} J(E')dE' \quad (4\text{-}3)$$

Here B_1 is adjusted to give same intensity of $J(E)$ at exactly 30 eV below the peak energy. Then the in-depth distribution of atoms can be estimated from the rules Table 1 using B_1 and A_p as the peak area of photoelectron peak [27].

The decay length L is determined from equation (4-4) when the distribution of atoms is either constant or exponentially varying with depth.

$$L = \frac{B_1}{B_0 - B_1} \lambda \cos\theta \quad (4\text{-}4)$$

Here $B_0 = 3000\,eV^2$, λ is the IMFP, θ is the emission angle of photoelectrons with respect to the surface normal. The in-depth distribution of atoms can then be estimated from Table 2. The QUASES software can be applied to model a rectangular or buried layer, island growth/overlayer, island growth/substrate, exponential profile or delta layer profile [28].

Furthermore, Hajati et al. has shown that it is possible to generate XPS 3D imaging using peak shape analysis applied to the spectral data stored in each pixel of a XPS imaging data set [29-31].

5. Composition Depth Profiling by ARXPS

ARXPS may be a good non-destructive analysis method to estimate the layer ordering of thin films. However, the estimation of depth profiles from ARXPS results is usually not simple because the signal from deeper depths (usually at low emission angles) always contains the signal from shallower depths. The angle profile can be estimated from the depth profile using the Emission Depth Distribution Function (EDDF), and the angle profile can then be compared with the obtained ARXPS results using an iterative calculation process. When the thin film including the substrate near the interface is divided into a total of p layers with each layer having a thickness of B, as shown in Fig.1, the signal intensity I_A of element A is expressed as equation (5-1).

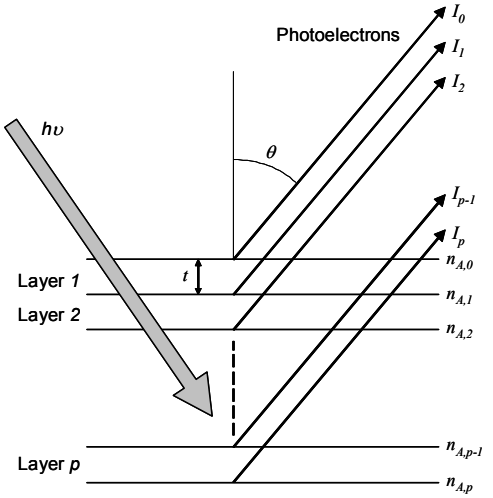

Fig. 1 Graphic illustration of the model used to generate ARXPS data. The I_0 emitted from the top surface is assumed to undergo no scattering.

$$I_A(\theta) = KS_A L_A(\alpha) \sum_{i=0}^{p} \left[n_{A,i} \exp\left(\frac{-t}{\lambda_{A,i} \cos\theta} \right) \right]^i \quad (5\text{-}1)$$

$$L_A(\alpha) = 1 + \frac{1}{2}\beta_A \left(\frac{3}{2}\sin^2\alpha - 1 \right) \quad (5\text{-}2)$$

Here K is the constant including the X-ray intensity, S_A is the relative sensitivity factor for the element A, $L_A(\alpha)$ is the asymmetry term excluding elastic scattering, α is the angle between incident X-ray and emission direction of the photoelectron, β_A is the asymmetry parameter, and $\lambda_{A,i}$ is the IMFP in the i th layer (e.g. $\lambda_{A,0}$ is IMFP for the vacuum). The measured atomic concentration of element A is at emission angle θ expressed as equation (5-3), when the thin film contains N elements.

$$X_A(\theta) = \frac{I_A(\theta)/S_A}{\sum_{j=A}^{N} I_j(\theta)/S_j} \quad (5\text{-}3)$$

The estimated angle profile can be simulated from equation (5-1) and (5-2) by changing the elemental distribution of the initial depth profile and comparing with the measured angle profile.

The linear least squares method or regularization method is generally applied to the simulation, but there may be problems, e.g. the intensity of the data is limited and the uncertainty of the signal is treated the same for the data from all angles. The MEM may be a more suitable tool for estimating a self-consistent result from a limited data set [32]. Smith et al. [3] had applied the MEM approach to ARXPS data from SiO_2 and TiN thin film layers and has reconstructed the depth profiles.

Skilling and Gull [33] defined the entropy in equation (5-4).

$$S = \sum_{j=1}^{N} \sum_{i=0}^{p} \left[n_{j,i} - m_{j,i} - n_{j,i} \log\left(n_{j,i} / m_{j,i} \right) \right] \quad (5\text{-}4)$$

Here $n_{j,i}$ is the simulated atomic concentration of element j in i th layer, and $m_{j,i}$ is the initial atomic concentration of element j in i th layer. The MEM solution can be obtained by maximizing

the entropy S when the chi-squared χ^2 expressed in equation (5-5) is within the uncertainty of measured ARXPS data.

$$\chi^2 = \sum_{j=1}^{N}\sum_{k=1}^{Nth}\frac{\left(c_{j,k}^{calc} - c_{j,k}^{obs}\right)^2}{\sigma_{j,k}^2} \quad (5\text{-}5)$$

Here $c_{j,k}^{calc}$ and $c_{j,k}^{obj}$ are the calculated values and the observed values of the atomic concentration of element j at angle k, respectively. These conditions can be met simultaneously by maximizing the joint logarithmic probability function Q expressed as equation (5-6).

$$Q = \alpha S - \chi^2/2 \quad (5\text{-}6)$$

Here α is the Lagrange multiplier (or regularizing parameter). A large value of α will result in an over-smoothed solution which is not in good agreement with the data. A small value of α will lead to over-fitting the data by attempting to reproduce the noise in the data. The measured angle profile may have a small change from a change of the depth profile of a thin film, so that calculated solutions at a localized minimum are easily obtained. Therefore, the following issues should be considered for MEM optimizations.

(1) Two or more initial estimates of the depth profiles can be compared [3]. Particularly, optimizations of the parameters using prior information about the films are extremely important.
(2) The Bayesian statistical analysis can be used to determine the overall scaling of the noise in the experimental data, thus avoiding the need to estimate the point at which to stop the calculation with the maximum entropy solution [3].
(3) Other methods, such as Rutherford Backscatter Spectroscopy (RBS) can be compared with the ARXPS results [34, 35].

6. XPS Depth Profiling of Organic Materials by Cluster Ion Beam

While the non-destructive analysis for ultra thin film such as gate oxides has been reviewed in the previous sections, destructive sputter depth profiling is also a useful method for organic materials (soft materials) such as multi-coatings on glass, OLEDs etc., when the thickness of the thin film is on the order of 100 nm [7]. Severe sample damage is observed on the surface of the sputter ablated samples when an Ar^+ ion beam is used for sputtering soft materials. This has previously hindered the depth profiling of chemical compositions and chemical states of soft materials. Recently, the cluster beam technology such as C_{60} has become commercially available, so that depth profiling of organic materials could be performed with minimum sample damage [8, 9]. However the carbon residue originating from the C_{60} cluster beam can limit the number of practically useable materials for cluster beam depth profiling [36]. The development of Ar cluster beam [37] and water droplet cluster ion beam have also attracted research interest [10, 11].

On the other hands, Shyue et al. have shown depth profiling of organic materials without carbon residue by using a 0.2 keV Ar ion beam and 10 keV C_{60} ion beam co-sputtering technique [38]. This has shown practical significance with the demonstrated chemical state depth profiling on 230 nm thick OLED and 485 nm thickness polymer solar cell samples.

7. Summary

An overview of thin film analyses such as the film thickness analysis of an overlayer thin film, the structure analysis of a multilayered thin film, the background shape analysis for thin films with a varying depth distribution and the compositional depth profile by ARXPS utilizing the maximum entropy method has been described. The depth profiling of organic thin films (such as ~100 nm in thickness) by cluster ion beam was also described as a destructive analysis. The film thickness analysis has also been developed as a 2D analysis, e.g. oxide thickness distribution on 200 mm silicon wafers [39]. The structure analysis by two emission angle may be used for the evaluation of chemically modified surfaces on the substrates [40]. The background analysis method is also useful for the evaluation of both homogeneous and structured thin films in short time compared with ARXPS measurements. However it is very challenging to optimize all the parameters in the QUASES software without including prior information about the film thickness. The MEM method has been applied in ARXPS for many thin films with optimizations of the MEM parameters [42-46]. The surface roughness [45, 47], the elastic scattering [34, 48], IMFP for chemical compounds [41], crystallization etc. need to be considered in all methods. Furthermore, since more EAL values should be estimated from the EDDF calculated by approaches such as quantum scattering theory [49], it is important to develop electron transport simulators for practical use in electron spectroscopy.

8. References

[1] C. S. Fadley et al., J. Electron Spectrosc. Relat. Phenom., **4**, 93 (1974).
[2] Semiconductor Industry Association, 2007 International Technology Roadmap for Semiconductors. http://public.itrs.net/.
[3] G. C. Smith and A. K. Livesey, Surf Interface Anal., **19** 175 (1992).
[4] H. Kato et al., Appl. Surf. Sci., **190**, 39 (2002).
[5] M. Nakamura et al., J. Surf. Anal., **12**, 263 (2005).
[6] S Tougaard, Surf. Interface Anal., **26**, 249 (1998).
[7] ISO 18115: Surface Chemical Analysis – Vocabulary, (International Organization for Standardization, Genève, Switzerland) 2001
ASTM E 673-95a, *Standard terminology relating to surface analysis*.
[8] N. Sanada, A. Yamamoto, R. Oiwa and Y. Ohashi, Surf. Interface Anal., **36**, 280 (2004).
[9] D. Sakai et al., J. Surf. Sci., **12**, 97 (2005).
[10] Y. Iijima et al., J. Surf. Anal., **14**, 437 (2008).
[11] Y. Sakai et al., J. Surf. Anal., **14**, 466 (2008).
[12] e.g. P. J. Cumpson, "Angle-Resolved X-Ray Photoelectron Spectroscopy in Surface Analysis by Auger and X-ray Photoelectron Spectroscopy", edited by D. Briggs and J. T. Grant, IM Publications and Surface Spectra Limited, 2003, pp 651-675.
[13] J. Hill, D. G. Royce, C. S. Fadley and L. F. Wagner, Chem. Phys. Letters, **44**, 225 (1976).
[14] M. P. Seah and S. J. Spencer, Surf. Interface Anal., **35**, 515 (2003).
[15] M. P. Seah and S. J. Spencer, Surf. Interface Anal., **33**, 640 (2002).
[16] P. J. Cumpson, Surf. Interface Anal., **29**, 403 (2000).
[17] [19] P. J. Cumpson, Surf. Interface Anal., **25**, 447 (1997).
[18] A. Jablonski and C. J. Powell, J. Vac. Sci Technol., **A15**, 2095 (1997).
[19] M. P. Seah et al., Surf. Interface Anal., **36**, 1269 (2002).
[20] M. Seah, J. Surf. Anal., **12**, 70 (2005).
[21] M. Seah, J. Surf. Anal., **13**, 136 (2006).
[22] M. P. Seah and S. J. Spencer, Surf. Interface Anal., **33**, 960 (2002).
[23] S. Tanuma, C. J. Powell and D. R. Penn, Surf. Interface Anal., **21**, 165 (1994).
[24] M. Seah, Surf. Interface Anal, **21**, 336 (1994).
[25] MultiPak AES & XPS Data Reduction Software Ver. 8.2C (2007) by ULVAC-PHI INC., 370 Enzo, Chjgasaki, 253-8522, Japan. See http://www.ulvac-phi.com/.
[26] S. Tougaard, Surf. Interface Anal., **25**, 137 (1997).
[27] S. Tougaard, "Quantification of Nano-structures by Electron Spectroscopy", edited by D. Briggs and J. T. Grant, IM Publications and Surface Spectra Limited, 2003, pp 295-343.
[28] S. Tougaard, QUASES: Software package for Quantitative XPS/AES of Surface Nanostructure by Peak Shape Analysis, Ver 5.1 (2002). See http://www.quases.com/.
[29] S. Hajati et al., Surf. Sci., **600**, 3015 (2006).
[30] S. Hajati et al., Surf. Sci., **602**, 3064 (2008).
[31] S. Hajati et al., Surf. Interface Anal., **40**, 688 (2008).
[32] D. G. Childers : Modern Spectral Analysis, (IEEE Press, New York, 1978).
[33] J. Skilling and S. F. Gull, IEE Porc. Prart F, **131(6)**, 646 (1984).
[34] K. Kimura et al., Surf. Interface Anal., **40**, 423 (2007).
[35] S. V. Merzlikin et al., Surf, Sci., **602**, 755 (2006).
[36] N. Sanada, private communication.
[37] T. Seki et al., Nucl. Instr. and Meth. in Phys. Res. **B206**, 902 (2003).
[38] B.-Y. Yu et al., Anal. Chem. **80**, 3412 (2008).
[39] e.g. C Thomas Larson, Emir Gurer, and J. Kelly Truman, "Using an XPS-based metrology system to determine film thickness and composition", Micro Magazine (2007). See http://www.micromagazine.com/archive/05/04/larson.html.
[40] T. Shirao et al., "Recent Developments and Application in XPS", Asian Pacific Conference on Surface Science & Engineering, Hong Kong Baptist Univ., China, December 19, (2006).
[41] G. Saheli et al., "Comparison of AR-XPS and Tougaard Methods for SiON Thin Film Characterization", 47th IUVSTA Workshop on Angle-Resolved XPS, Riviera Maya, Mexico, March 26-30, (2007).
[42] P. Cumpson, "Overcoming Ill-Conditioning", 47th IUVSTA Workshop on Angle-Resolved XPS, Riviera Maya, Mexico, March 26-30, (2007).
[43] A. Mathew and R. L. Opila, "What Angle-Resolved Photoemission Can Tell Us About High-K Dielectrics Using the Maximum Entropy Algorithm", 47th IUVSTA Workshop on Angle-Resolved XPS, Riviera Maya, Mexico, March 26-30, (2007).
[44] S. Oswald and F. Oswald, Surf. Interface Anal., **40**, 700 (2008).
[45] S. Oswald, Surf. Sci. **602**, 291 (2008).
[46] Z. Chanbi and R. W. Paynter, J. Electron

Spectrosc. Relat. Phenom, **164**, 28 (2008).
[47] e.g. A. I. Mart´ın-Concepción, F. Yubero, J. P. Espinón and S. Tougaard, Surf. Interface Anal., **36**, 788 (2004).
[48] e.g. T. Fujikawa et al., J. Electron Spectrosc. Relat. Phenom, **151**, 170 (2006).
[49] H. Shinotsuka et al., Pys. Rev. B **77**, 085404 (2008).